

Nucleon resonances in $\pi N \rightarrow \eta' N$ and $J/\psi \rightarrow p\bar{p}\eta'$ *

Xu Cao(曹须)^{1,2,3,4;1)} Ju-Jun Xie(谢聚军)^{1,2,3,4;2)}

¹ Institute of Modern Physics, Chinese Academy of Sciences, Lanzhou 730000, China

² State Key Laboratory of Theoretical Physics, Institute of Theoretical Physics,
Chinese Academy of Sciences, Beijing 100190, China

³Kavli Institute for Theoretical Physics China (KITPC), Chinese Academy of Sciences, Beijing 100190, China

⁴Research Center for Hadron and CSR Physics, Institute of Modern Physics of
CAS and Lanzhou University, Lanzhou 730000, China

Abstract: We are aiming to study the $J/\psi \rightarrow p\bar{p}\eta'$ decay in an isobar model and the effective Lagrangian approach on the basis of the coupling constants extracted from the $\pi N \rightarrow \eta' N$ reaction. After a careful exploration of the contributions of the $S_{11}(1535)$, $P_{11}(1710)$, $P_{13}(1900)$, $S_{11}(2090)$ and $P_{11}(2100)$ resonances, we conclude that either a subthreshold resonance or a broad P-wave state in the near threshold range seems to be indispensable to describe the present data of the $\pi N \rightarrow \eta' N$. Furthermore, at least one broad resonance above $\eta' N$ threshold is preferred. With this detailed analysis, we give the invariant mass spectrum and Dalitz plot of the $J/\psi \rightarrow p\bar{p}\eta'$ decay for the purpose of assisting the future detailed partial wave analysis. It is found that the $J/\psi \rightarrow p\bar{p}\eta'$ data are useful for disentangling the above or below threshold resonant contribution, though it still further needs the differential cross section data of $\pi N \rightarrow \eta' N$ to realize some of the resonant and non-resonant contribution.

Keywords: nucleon resonances, isobar model, partial wave analysis

PACS: 13.20.Gd, 13.75.Gx, 14.20.Gk **DOI:** 10.1088/1674-1137/40/8/083103

1 Introduction

In recent years, plenty of information on nucleon resonances [1] has been obtained by a wealth of phenomenological studies on numerous data of the πN , γN , eN reactions [2–22] and pN collisions [23–35]. However, despite a great deal of theoretical and experimental effort, our knowledge of nucleon resonances around 2.0 GeV is still scarce because of the presence of many resonances and opening channels in this energy region. Alternatively, the hadronic decay channels of heavy quarkonium have attracted much attention due to their advantage in extracting empirical information of resonances with isospin 1/2. In this area, a lot of progress has been made on the study of the decay of the charmonium states, e.g. the J/ψ , $\psi(3686)$, $\psi(3770)$ and χ_{cJ} states by the BES and CLEO collaborations [36–46]. In particular, it is advanced by the wide implementation of the tools of partial wave analysis (PWA) [47–49] on the tremendous number (up to a billion) of events accumulated with the BESIII detector at the BEPCII facility. In these fruitful PWA works, which mainly concentrate on the $N\bar{N}\pi$ channels, not only have the peaks of known N^* resonances been directly observed, but evidence of several new resonances

with higher masses has also been found [36–38], e.g. $N^*(2040)$ with $J^P = 3/2^+$ was found in $J/\psi \rightarrow p\bar{p}\pi^0$ [36], $N^*(2300)$ with $J^P = 1/2^+$ and $N^*(2570)$ with $J^P = 5/2^-$ appeared in $\psi(3686) \rightarrow p\bar{p}\pi^0$ [38].

It is indispensable to explore the decay modes with final mesons other than the π -meson in order to search for missing states coupling weakly to the π -meson. Unfortunately, to date we know little about the coupling of the η' -, ω -, and ϕ -mesons to nucleon resonances [50] and the interaction of these mesons with the nucleon [51]. In past decades, the production of these mesons in the γN and pN reactions have been widely investigated, mainly motivated by the increasing volume of data taken by the CLAS, CBELSA and COSY groups [24–31, 52–55]. The results, however, are quite inconclusive for the moment. It is still not firmly established which resonances play an important role in these reactions, and it is still controversial whether the sub-threshold resonances have essential contributions. In order to resolve these ambiguities, it is natural to turn our attention to the strange decays of charmonium states, e.g. $N\bar{N}\eta'$, $N\bar{N}\phi$, and the associate strange decay channels $N\bar{N}K$ and $N\bar{N}K^*$ [42].

The invariant mass spectra of the $J/\psi \rightarrow N\bar{N}\eta'$ decays cover the energy range from $m_N + m_{\eta'} \simeq 1.90$ GeV

Received 10 September 2015, Revised 12 April 2016

* Supported by National Natural Science Foundation of China (11347146, 11405222, 11105126, 11475227)

1) E-mail: caoxu@impcas.ac.cn

2) E-mail: xiejujun@impcas.ac.cn

©2016 Chinese Physical Society and the Institute of High Energy Physics of the Chinese Academy of Sciences and the Institute of Modern Physics of the Chinese Academy of Sciences and IOP Publishing Ltd

to $m_{J/\psi} - m_N \simeq 2.16$ GeV, where the debatable $P_{13}(1900)$ state [4, 7] and the long-sought third S_{11} and P_{11} states at about 2100 MeV [2–7] are expected to be present. The $P_{13}(1900)$ state, which is unfavored by diquark models, is considered at the early stage of the Giessen model [7–11] and KSU survey [14, 15]. The Bonn-Gatchina partial wave analysis found evidence for it in the $K\Sigma$ photoproduction data only recently [3, 4], but the latest GWU analysis does not include it as before [16]. The existence of the third S_{11} and P_{11} states could shed light on the spin quartet of nucleon resonances, which is disputed in classical diquark models [5]. This topic is interesting also because it could shed light on the nature and internal structure of relevant nucleon resonances which may have large $s\bar{s}$ components [50]. It can also serve as a guideline for future detailed PWA in view of the current scarce information on these resonances.

In the decay channels mentioned, the possible background contribution, e.g. the nucleon pole, has been calculated to be negligible, except in $J/\psi \rightarrow N\bar{N}\pi$ [56–58], as anticipated by the suppression from the large off-shell effect. The meson-pole Feynman diagrams, e.g. $J/\psi \rightarrow M\eta' \rightarrow (p\bar{p})\eta'$, can also be ignored because of the smallness of the relevant coupling [59]. So the main contribution should come from the nucleon resonances. In an isobar model including several possible resonances coupling strongly to $N\phi$, $J/\psi \rightarrow p\bar{p}\phi$ has been studied and useful hints are given for the future data analysis [60]. In this paper, we will give a full study of the $J/\psi \rightarrow p\bar{p}\eta'$ decay based on our present understanding of the resonances with mass around 2.0 GeV with the model parameters constrained by the data of the $\pi N \rightarrow \eta'N$ channel.

η' -meson photoproduction is complicated by large contributions of the t-channel exchange and contact term from gauge invariance. As a result, more parameters are needed in the analysis of these reactions. The conclusions after including these data, especially the masses of the S- and P-wave states, are very different in the series of works [52–55]. This tells us that the background contribution should be treated carefully in the photoproduction, which is another important issue in the study of η' -meson production. This also motivates our present study, which is devoted to a simpler case of πN reactions and J/ψ decay with less background. The η' -meson production in nucleon-nucleon reactions now has close-to-threshold data. The old data have been analyzed in our previous work [30], and the conclusion is compatible with our present work. But these data cannot determine well the mass and width of the contributing S_{11} resonance because the phase space behavior is dominant at the close-to-threshold region. Another motivation of this paper is to check if the J/ψ decay could give us more information in this aspect.

In the next section, the construction of the model and the mathematical framework are presented in detail. Section 3 gives the calculated results, followed by a short summary in Section 4.

2 Ingredients and formalism

We use the isobar model with the assumption of nucleon resonance dominance. We use the available data of the $\pi N \rightarrow \eta'N$ reaction to determine the unknown coupling constants of $\eta'NN^*$ vertices. The s- and u-channel process as depicted in Fig. 1 are included in the model, but the t-channel contribution is not considered because we do not find any mesons coupling strongly to $\pi\eta'$. For example, the width of the $\eta' \rightarrow \rho\pi$ decay is smaller than 8.0 keV [1]. The nucleon pole [55] is calculated to be very small so we disregard it, too. As pointed out above, the invariant mass of $\eta'N$ and $\eta'\bar{N}$ in the $J/\psi \rightarrow p\bar{p}\eta'$ decay cover the energies up to 2.16 GeV, so herein we consider the center of mass (c.m.) energy range from threshold to 2.5 GeV in the $\pi N \rightarrow \eta'N$ reaction in order to better constrain the coupling constants of the $\eta'NN^*$ vertices. The Feynman diagrams of the $J/\psi \rightarrow p\bar{p}\eta'$ decay in the model are shown in Fig. 2. We use the experimental branching ratios (BR) of $J/\psi \rightarrow p\bar{p}\eta$ and $J/\psi \rightarrow p\bar{p}\pi^0$ to extract the coupling constants of $J/\psi NN^*$, whose Feynman diagrams are similar to Fig. 2, but replacing the final meson by the π - and η -meson, respectively.

Before continuing to the formalism, we first explain the strategy of selecting the nucleon resonances in the model. We only include the S- and P-wave states because the energy we consider here is not far away from threshold, and also there is little evidence of higher spin resonances coupling to $\eta'N$ [1]. A further reference worthy of mention is that PWA of $J/\psi \rightarrow p\bar{p}\eta$ does not find any signal of higher partial waves [40]. In addition, we consider the known states with relatively big partial decay widths to be strange or associated strange channels, because these states are expected to couple strongly to the $\eta'N$ channel. The $P_{13}(1900)$ state, located very close to the $\eta'N$ threshold, seems to have big couplings to ηN , $K\Sigma$, $K\Lambda$ [1] and $N\phi$ [60]. However its decay width to $\eta'N$ is critically suppressed by the very small phase space, which is probably the reason for its obscurity in the present PWA analysis. Just above the threshold is situated the $S_{11}(2090)$ and $P_{11}(2100)$, which may have big couplings to $\eta'N$ but rank only two and one star, respectively, in the compilation of the Particle Data Group (PDG) [1]. The $S_{11}(2090)$ is labeled as $S_{11}(1895)$ in the latest PDG with the recommended Breit-Wigner mass being around 2090 MeV. We include the sub-threshold resonance $S_{11}(1535)$ because it may have big couplings to $\eta'N$, as found in the $pN \rightarrow pN\eta'$ reaction [30]. In fact, the constituents of this resonance may have significant $s\bar{s}$ element [61, 62], resulting in its big couplings to $K\Lambda$ [23]

and $N\phi$ [25, 31, 63]. However, the combination of several S- and P-wave resonances above the $\eta'N$ threshold could give a reasonable description of the $pN \rightarrow pN\eta'$ data [52–55]. One of the purposes of this paper is to explore whether it is possible to discriminate these two η' production mechanisms in the $J/\psi \rightarrow p\bar{p}\eta'$ decay. Another sub-threshold resonance $P_{11}(1710)$ is considered in the model because it has a relatively big decay width to the ηN . Other sub-threshold resonances, i.e. the $S_{11}(1650)$ and $P_{11}(1880)$ states [1, 3] are not considered because they cannot be distinguished from the nearby $S_{11}(1535)$ and $P_{11}(1710)$ resonances by the current η' production data. So in this paper we include $S_{11}(1535)$, $P_{11}(1710)$, $P_{13}(1900)$, $S_{11}(2090)$ and $P_{11}(2100)$, labeled as 1 – 5 with increasing masses. As can be seen in the PDG [1], the widths of the last three resonances have a big discrepancy between different models. Herein we adopt the treatment in Ref. [60] and use three widths for each resonance, determined by three different models [1], labeled respectively as (a), (b) and (c) from narrow to wide. We try to use the combinations of these widths to fit the data with fewer model parameters. In the following text, we label different fitting strategies as nr.ixjy kz, which means fitting with n resonances with the (x)-th, (y)-th and (z)-th widths for the i -th, j -th and k -th resonances, respectively. For example, 3r.2-3b4c is fitting with 3 resonances, which are $P_{11}(1710)$, $P_{13}(1900)$ with its (b) width, and $S_{11}(2090)$ with its (c) width.

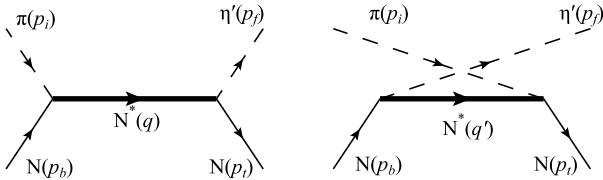


Fig. 1. The s- and u-channel Feynman diagram for the $\pi N \rightarrow \eta' N$ reaction in the isobar model.

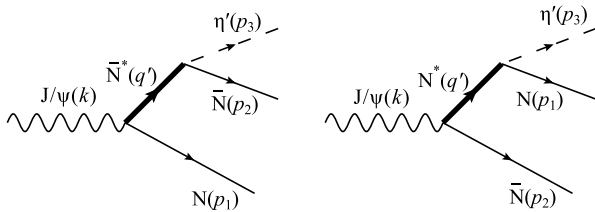


Fig. 2. The Feynman diagram for the $J/\psi \rightarrow p\bar{p}\eta'$ decay in the isobar model.

In order to evaluate the Feynman diagrams in Figs. 1 and 2, we construct the effective Lagrangians with the covariant L - S (orbital-spin) coupling scheme [33, 34, 47–49]. The couplings of the pseudoscalar meson ($M = \tau, \pi$, η or η') to S_{11} , P_{11} and P_{13} resonances (R) are:

$$\mathcal{L}_{MNR}^{1/2\pm} = g_{MNR} \bar{N} \Gamma^\pm M R + \text{h.c.}, \quad (1)$$

$$\mathcal{L}_{MNR}^{3/2+} = i \frac{g_{MNR}}{m_R} \bar{N} \partial^\mu M R_\mu + \text{h.c.}, \quad (2)$$

with $\Gamma^- = 1$ and $\Gamma^+ = i\gamma_5$ for $R = S_{11}$ and P_{11} , respectively. The couplings of the J/ψ to resonances are:

$$\mathcal{L}_{\psi NR}^{1/2\pm} = g_{\psi NR} \bar{N} \Gamma_\mu^\pm \epsilon^\mu(\mathbf{p}_\psi, s_\psi) R + \text{h.c.}, \quad (3)$$

$$\mathcal{L}_{\psi NR}^{3/2+} = i g_{\psi NR} \bar{N} \gamma_5 \epsilon^\mu(\mathbf{p}_\psi, s_\psi) R_\mu + \text{h.c.}, \quad (4)$$

with $\Gamma_\mu^- = i\gamma_5 \sigma_{\mu\nu} p_\psi^\nu / m_N$ and $\Gamma_\mu^+ = \gamma_\mu$ for $R = S_{11}$ and P_{11} , respectively. It should be noted that the J/ψ produced in e^+e^- collisions is transversely polarized so the polarization vector $\epsilon_\mu(\mathbf{p}, s_\psi)$ satisfies

$$\sum_{s_\psi = \pm 1} \epsilon_\mu(\mathbf{p}, s_\psi) \epsilon_\nu^*(\mathbf{p}, s_\psi) = \delta_{\mu\nu} (\delta_{\mu 1} + \delta_{\mu 2}). \quad (5)$$

The intermediate resonances are multiplied by off-shell form factors to suppress the contribution of high momentum:

$$F_R(q^2) = \frac{\Lambda_R^4}{\Lambda_R^4 + (q^2 - m_R^2)^2}, \quad (6)$$

with Λ_R and q being, respectively, the cut-off parameter and four-momentum of the resonances. $\Lambda_R = 1.1$ GeV and 2.0 GeV are used in the s- and u-channel in the $\pi N \rightarrow \eta' N$ reaction, respectively. Here we use bigger cut-off values of the u-channel in order to reproduce the large cross section data of $\pi N \rightarrow \eta' N$ above 2.3 GeV, as will be discussed in the next section. In the J/ψ decay channels, $\Lambda_R = 1.8$ GeV and 2.3 GeV are adopted for the resonances below and above threshold, respectively. The propagators of the resonances with total spin $J = 1/2$ and $3/2$ are:

$$G_R^{1/2}(q) = \frac{-i(q \pm m_R)}{q^2 - m_R^2 + im_R \Gamma_R}, \quad (7)$$

$$G_R^{3/2}(q) = G_R^{1/2}(q) G_{\mu\nu}(q), \quad (8)$$

$$G_{\mu\nu}(q) = -g_{\mu\nu} + \frac{1}{3} \gamma_\mu \gamma_\nu \pm \frac{1}{3m_R} (\gamma_\mu q_\nu - \gamma_\nu q_\mu) + \frac{2}{3m_R^2} q_\mu q_\nu, \quad (9)$$

where \pm are for the particles and antiparticles, respectively.

The partial decay widths of nucleon resonances can be calculated by the above Lagrangians, e.g. Eq. (1) and Eq. (2) as follows:

$$\Gamma_{R \rightarrow NM} = \frac{g_{MNR}^2 (E_N \pm m_N) p_N^{\text{cm}}}{4\pi m_R} \Gamma_J \Gamma_M, \quad (10)$$

$$E_N = \frac{m_R^2 + m_N^2 - m_M^2}{2m_R}, \quad (11)$$

$$p_N^{\text{cm}} = \sqrt{E_N^2 - m_N^2}, \quad (12)$$

with $\Gamma_{1/2} = 1$, $\Gamma_{3/2} = (p_N^{\text{cm}}/m_R)^2$, $\Gamma_\pi = 3$ and $\Gamma_\eta = 1$. The \pm is for S_{11} (P_{13}) and P_{11} , respectively. So the coupling constants of vertex MNR , as listed in Table 1,

can be determined by the experimental decay widths of $R \rightarrow NM$ in the compilation of PDG [1]. Because the parameters of $P_{13}(1900)$, $S_{11}(2090)$ and $P_{11}(2100)$ have large uncertainties, their widths are adopted from three

PWA groups, see PDG [1] for details. The branching decay ratio of $S_{11}(1535)$ and $P_{11}(1710)$ to the ηN channel are 53% and 6.2%, respectively, with the resulting values $g_{\eta NN^*(1535)}^2 = 4.31$ and $g_{\eta NN^*(1710)}^2 = 3.14$.

Table 1. The parameters of nucleon resonances used in the calculation. The Breit-Wigner masses, widths and branching ratios (BR) are quoted from the central values of the PDG [1].

label	N^*	mass/MeV	$\Gamma_{\text{tot}}/\text{MeV}$	$BR_{\pi N}(\%)$	$g_{\pi NR}^2$	$\Gamma_{J/\psi NN^*}/\text{keV}$	$g_{\psi NR}^2(10^{-5})$
1	$S_{11}(1535)$	1530	137.5	45.0	0.47	9.94×10^{-2}	0.652
2	$P_{11}(1710)$	1695	75.0	15.0	1.08	1.23×10^{-2}	0.316
3	$P_{13}(1900)$	1900	(a) 180.0	5.5	1.13	1.23×10^{-2}	2.422
			(b) 250.0	10.0	2.85	1.23×10^{-2}	1.475
			(c) 498.0	26.0	14.7	1.23×10^{-2}	0.774
4	$S_{11}(2090)$	2090	(a) 95.0	9.0	0.041	1.23×10^{-2}	22.05
			(b) 350.0	18.0	0.305	1.23×10^{-2}	7.521
			(c) 414.0	10.0	0.200	1.23×10^{-2}	13.20
5	$P_{11}(2100)$	2100	(a) 113.0	15.0	0.564	1.23×10^{-2}	1.362
			(b) 200.0	10.0	0.666	1.23×10^{-2}	2.290
			(c) 260.0	12.0	1.040	1.23×10^{-2}	2.031

After some algebraic manipulation, the separate amplitudes of the $\pi^\pm N \rightarrow \eta' N$ are written as,

$$\begin{aligned} \mathcal{M}_R = & \sqrt{2} g_{\eta' NR} g_{\pi NR} \times \\ & [e^{i\phi_s} F_R(q) \bar{u}(p_t) \Gamma_{\eta' NR} G_R(q) \Gamma_{\pi NR} u(p_b) \\ & + e^{i\phi_u} F_R(q') \bar{u}(p_t) \Gamma_{\pi NR} G_R(q') \Gamma_{\eta' NR} u(p_b)], \end{aligned} \quad (13)$$

with $q = p_b + p_i$ and $q' = p_b - p_f$ for s- and u-channel, respectively. Here the interaction vertices $\Gamma_{\eta' NR}$ and $\Gamma_{\pi NR}$ can be read directly from Eq. (1) and Eq. (2) as 1, $i\gamma_5$ and $ip_{f,i}^\mu/m_R$ for $R = S_{11}$, P_{11} and P_{13} respectively. The total amplitude is the coherent sum of all resonances with the relative phase setting as free parameters to be determined by the data.

The $J/\psi \rightarrow N\bar{N}M$ ($M = \pi$ or η') decay amplitude for each resonance can be written as,

$$\begin{aligned} \mathcal{M}_R = & \delta_M e^{i\phi_s} g_{MNR} g_{\psi NR} \\ & \times [F_R(q) \bar{v}(p_2) \Gamma_{MNR} G_R(q) \Gamma_{\psi NR} \epsilon^\mu(\mathbf{p}_\psi, s_\psi) \bar{u}(p_1) \\ & + F_R(q') \bar{u}(p_1) \Gamma_{MNR} G_R(q') \Gamma_{\psi NR} \epsilon^\mu(\mathbf{p}_\psi, s_\psi) v(p_2)], \end{aligned} \quad (14)$$

with the isospin factor $\delta_M = 1$ or $\sqrt{2}$ for neutral or charged final mesons, respectively. The vertices $\Gamma_{\psi NR}$ can be read directly from Eq. (3) and Eq. (4) as $i\gamma_5 \sigma_{\mu\nu} p_\psi^\nu/m_N$, γ_μ and $i\gamma_5$ for $R = S_{11}$, P_{11} and P_{13} respectively.

We use the same method to determine the $g_{\psi NR}$ as in Ref. [60] and update the values with the amplitudes in Eq. (14). In BES's PWA [40], the branching ratio of $J/\psi \rightarrow p\bar{p}\eta$ is determined to be $(1.91 \pm 0.02 \pm 0.17) \times 10^{-3}$, of which the $S_{11}(1535)$ contributes $(56 \pm 15)\%$. So the $g_{\psi NN^*(1535)}$ can be well determined, taking advantage of the above value of the $g_{\eta NN^*(1535)}$. Combining with the known $g_{\pi NN^*(1535)}$, we can predict that the

fraction contribution of the $S_{11}(1535)$ in $J/\psi \rightarrow p\bar{p}\pi^0$ is 1.83×10^{-2} keV, compatible with the branching fraction $(0.92 \sim 2.10) \times 10^{-4}$ in BES's PWA [36]. However, the contribution of other resonances in $J/\psi \rightarrow N\bar{N}M$ is not well disentangled by PWA and they depend on the model parameters and the selected sets of resonances [36]. The total branching ratio of the $J/\psi \rightarrow p\bar{p}\pi^- + c.c.$ is consistent with expectation from the $J/\psi \rightarrow p\bar{p}\pi^0$ with the isospin relation but the fraction contribution of separate resonances is not extracted yet [37]. Based on the uncertainties given by the BES analysis [36], we can safely assume that the fraction contribution of the $P_{11}(1710)$, $P_{13}(1900)$, $S_{11}(2090)$ and $P_{11}(2100)$ are all 10% in $J/\psi \rightarrow p\bar{p}\pi^0$, then the $g_{\psi NR}$ can be determined, as tabulated in Table 1. The extracted values are in the same order and compatible with the fact that the J/ψ decay is a flavor-blind gluon-rich process. These values are also a good starting point to calculate other J/ψ hadronic decay channels, e.g. the $J/\psi \rightarrow N\bar{N}\pi\pi$ channel.

3 Numerical results

In order to reliably control the u-channel contribution in the $\pi N \rightarrow \eta' N$ reaction, we include its data up to the center of mass (c.m.) energy $\sqrt{s} = 2.50$ GeV. After the parameters in the u-channel are pinned down at high energies, the contribution of s-channel resonances can be extracted with more confidence. The total cross section of $\pi N \rightarrow \eta' N$ is around 100 nb and roughly at the same level from the threshold to $\sqrt{s} = 2.50$ GeV [64]. The data also show an inconspicuous structure with two bumps at threshold and around 2.15 GeV, respectively. These prominent features are directly reflected in the following numerical fit results.

Evidently, one resonance alone cannot give an excellent description of the data in this wide energy range. However, the $P_{11}(1710)$ could achieve a fair χ^2 with the existing data, indicated as 1r.2- in Table 2. As demonstrated in Fig. 3, the u-channel $P_{11}(1710)$ diagram contributes a significant smooth background and the trend describes roughly the features of the data without a clear signal of generated resonances as mentioned above. At this stage we cannot exclude this possibility due to the scarce data collected. Adding other resonances located above threshold, either wide or narrow, could improve the fit quality of the data. Due to the large number of solutions if $P_{11}(1710)$ is included in the model, we only show some selected typical fitted parameters in Table 2, with the corresponding curves depicted in Fig. 3. We can see that the χ^2 gets a little better when the number of resonances increases. As shown in Fig. 3(c), the four-resonance solution gives a clear two-bump structure and is different from other solutions with relatively plain curves. But the five-resonance solution 5r.1-2-3c4c5c has nearly the same quality as the four-resonance one in terms of the χ^2 values, while the uncertainties in its parameters are obviously bigger, exhausting the limitation of the data. This is also one of the reasons why we do not include more resonances in our model. It is a common feature that the u-channel $P_{11}(1710)$ contribution acts as an important smooth background and other resonances induce broad humps in all these solutions.

In the following text we focus on the solution without the $P_{11}(1710)$ resonances. Two types of combination of two resonances have a good χ^2 . One is the $P_{11}(1710)$

with a resonance above threshold, with a representative example already shown as solution 2r.2-4c in Table 2 and Fig. 3(a). The other one is the $P_{13}(1900)$ and broad $P_{11}(2100)$, and the extracted parameters are presented in the upper part of Table 3, with a typical diagram of the total cross section of $\pi N \rightarrow \eta' N$ shown in Fig. 4(a). In the two-resonance solution, a relatively broad resonance above threshold is favored in order to reproduce the level behavior in the data. Here the $S_{11}(1535)$ seems not to be needed, but we should be cautious to draw this conclusion because the $S_{11}(1535)$ only contributes to the very close-to-threshold region, so adding only one resonance besides the $S_{11}(1535)$ cannot explain well the big cross section at high energy. Surely, the $S_{11}(1535)$ alone could give a reasonable account of the very close-to-threshold data, as discussed in Ref. [30] and shown in the three- and four-resonance solutions below.

Besides the three-resonance solution with the $P_{11}(1710)$, representatively shown in Fig. 3(b), all other three-resonance solutions with χ^2 around 2.3 are summarized in Table 3 and typical diagrams are shown in Fig. 4(b-d). As can be seen in Fig. 4(b)(c), the $N^*(1535)$ could improve the χ^2 from around 2.6 to about 2.3, mainly because of the better fit to the close-to-threshold data. However, its role could be substituted by other resonances above threshold and the combination of the $P_{13}(1900)$, $S_{11}(2090)$ and $P_{11}(2100)$ could give an equally good description of the data, as shown in Fig. 4(c). Obviously, we need more data to differentiate these mechanisms, especially those of the angular distributions and polarized observables.

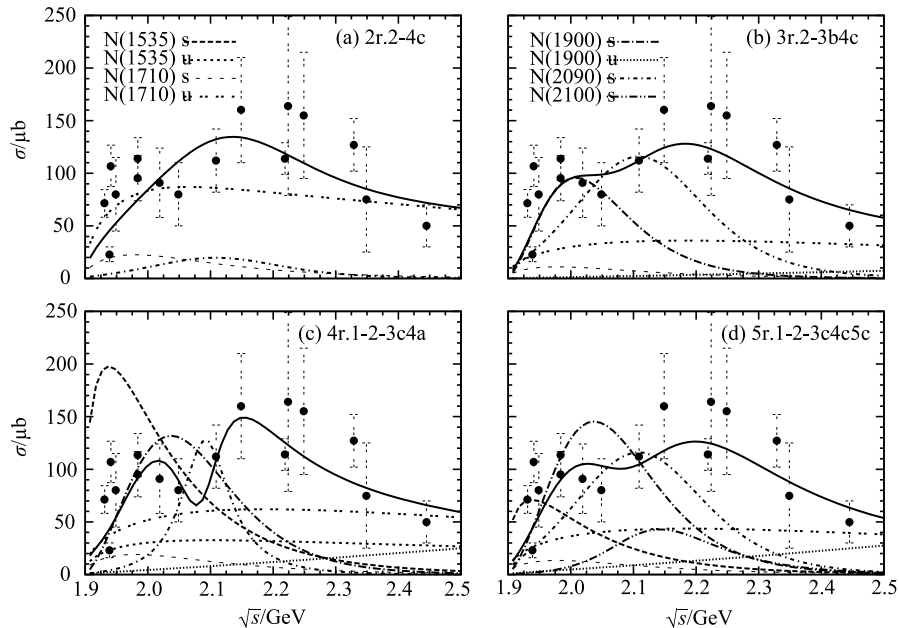


Fig. 3. Selected diagrammatic representation for the fitted results with $P_{11}(1710)$ included in the model. The solutions are labeled as 2r.2-4c, 3r.2-3b4c, 4r.1-2-3c4a and 5r.1-2-3c4c5c, see Table 2 for the corresponding parameters. The solid lines are the total contributions of all considered diagrams. The explanation of the meaning of other lines in the figures is indicated in Fig. (a) and Fig. (c). The data are from the compilation [64].

Table 2. The coupling constants of nucleon resonances to $\eta'N$ and relative phases extracted in the fit with $P_{11}(1710)$ included in the model. Only selected results are displayed, see the text for details. *: The values are set to be zero in the fit.

label/ χ^2	N*	width	$g_{\eta'NR}$	$\phi_s/(\circ)$	$\phi_u/(\circ)$
1r.2-/2.77	1710	—	12.97 ± 0.88	0.0*	123.8 ± 8.7
2r.2-4c	1710	—	9.95 ± 1.85	0.0*	128.9 ± 18.3
2.32	2090	(c)	0.71 ± 0.26	0.0 ± 274.6	156.5 ± 213.2
3r.1-2-5b	1535	—	3.02 ± 1.48	0.0*	138.8 ± 138.1
	1710	—	10.83 ± 2.37	0.0 ± 55.4	21.2 ± 58.5
2.36	2100	(b)	2.18 ± 1.39	43.0 ± 84.8	248.0 ± 119.0
3r.2-3b4c	1710	—	6.96 ± 2.25	0.0*	277.0 ± 77.9
	1900	(b)	12.37 ± 3.26	139.0 ± 89.5	1.5 ± 300.5
2.10	2090	(c)	1.73 ± 1.03	62.4 ± 64.5	297.7 ± 299.7
4r.1-2-3c4a	1535	—	9.48 ± 4.17	0.0*	0.9 ± 324.9
	1710	—	9.14 ± 1.22	0.0 ± 352.8	4.8 ± 242.8
	1900	(c)	10.06 ± 2.93	269.8 ± 106.8	359.9 ± 352.1
2.02	2090	(a)	0.93 ± 0.98	138.3 ± 80.0	1.7 ± 208.1
5r.1-2-3c4c5c	1535	—	5.68 ± 6.38	0.0*	1.6 ± 37.8
	1710	—	7.67 ± 2.87	31.2 ± 68.0	19.1 ± 41.1
	1900	(c)	10.56 ± 2.46	286.5 ± 104.7	8.3 ± 231.3
	2090	(c)	1.73 ± 1.36	146.1 ± 52.9	20.5 ± 348.9
2.06	2100	(c)	3.12 ± 3.80	0.1 ± 355.9	295.6 ± 86.3

Table 3. The coupling constants of nucleon resonances to $\eta'N$ and relative phases extracted in the fit with the combination of two or three resonances, mentioned as type I, see the text for details. *: The values are set to be zero in the fit.

label/ χ^2	N*	width	$g_{\eta'NR}$	$\phi_s/(\circ)$	$\phi_u/(\circ)$
2r.3a5c	1900	(a)	12.71 ± 2.07	0.0*	209.7 ± 101.1
2.65	2100	(c)	5.48 ± 0.72	151.3 ± 81.4	95.3 ± 97.8
2r.3b5c	1900	(b)	10.70 ± 1.76	0.0*	169.4 ± 86.2
2.61	2100	(c)	5.56 ± 0.81	118.2 ± 72.8	44.9 ± 84.4
2r.3c5c	1900	(c)	8.88 ± 1.37	0.0*	150.4 ± 62.4
2.63	2100	(c)	5.12 ± 1.05	98.5 ± 54.7	11.9 ± 198.9
3r.1-3b4b	1535	—	4.90 ± 2.38	0.0*	55.1 ± 59.4
	1900	(b)	13.02 ± 1.13	332.0 ± 58.5	242.9 ± 65.5
2.28	2090	(b)	1.37 ± 0.41	252.4 ± 24.5	57.2 ± 104.7
3r.1-3c4b	1535	—	3.59 ± 1.47	0.0*	247.5 ± 42.8
	1900	(c)	9.36 ± 1.19	138.2 ± 28.2	47.0 ± 38.6
2.28	2090	(b)	1.58 ± 0.31	0.0 ± 13.1	245.1 ± 89.9
3r.1-3a5c	1535	—	4.83 ± 1.94	0.0*	0.0 ± 19.5
	1900	(a)	14.49 ± 2.93	265.9 ± 51.4	155.4 ± 49.7
2.38	2100	(c)	5.79 ± 0.99	87.0 ± 52.3	2.5 ± 229.5
3r.1-3b5b	1535	—	5.36 ± 1.10	0.0*	0.0 ± 22.2
	1900	(b)	12.50 ± 1.77	264.1 ± 45.2	166.8 ± 38.6
2.43	2100	(b)	5.08 ± 1.00	122.6 ± 48.8	5.2 ± 70.2
3r.1-3b5c	1535	—	4.27 ± 1.37	0.0*	0.0 ± 47.4
	1900	(b)	10.01 ± 1.61	0.0 ± 53.4	171.0 ± 47.8
2.35	2100	(c)	5.32 ± 1.32	140.9 ± 61.2	4.0 ± 216.0
3r.1-3c5b	1535	—	5.85 ± 1.30	0.0*	0.0 ± 55.9
	1900	(c)	8.94 ± 1.92	305.4 ± 62.3	162.5 ± 56.3
2.29	2100	(b)	4.13 ± 1.48	117.8 ± 49.1	12.4 ± 208.1
3r.3b4b5c	1900	(b)	12.97 ± 1.05	0.0*	230.6 ± 67.3
	2090	(b)	0.91 ± 0.44	234.7 ± 36.9	70.3 ± 116.4
2.33	2100	(c)	4.91 ± 1.04	139.9 ± 62.6	91.9 ± 59.4
3r.3b4c5c	1900	(b)	13.04 ± 0.81	0.0*	225.5 ± 63.3
	2090	(c)	1.38 ± 0.44	235.7 ± 34.6	66.3 ± 108.5
2.31	2100	(c)	4.76 ± 1.03	130.9 ± 55.4	86.3 ± 56.5
3r.3c4b5c	1900	(c)	10.49 ± 0.89	0.0*	241.4 ± 53.6
	2090	(b)	1.15 ± 0.44	221.0 ± 26.0	90.3 ± 117.3
2.27	2100	(c)	4.33 ± 1.56	159.1 ± 61.0	108.9 ± 58.6
3r.3c4c5c	1900	(c)	10.53 ± 0.75	0.0*	219.3 ± 68.7
	2090	(c)	1.68 ± 0.75	219.8 ± 25.5	62.0 ± 207.5
2.29	2100	(c)	3.72 ± 1.77	141.5 ± 76.1	84.4 ± 88.9

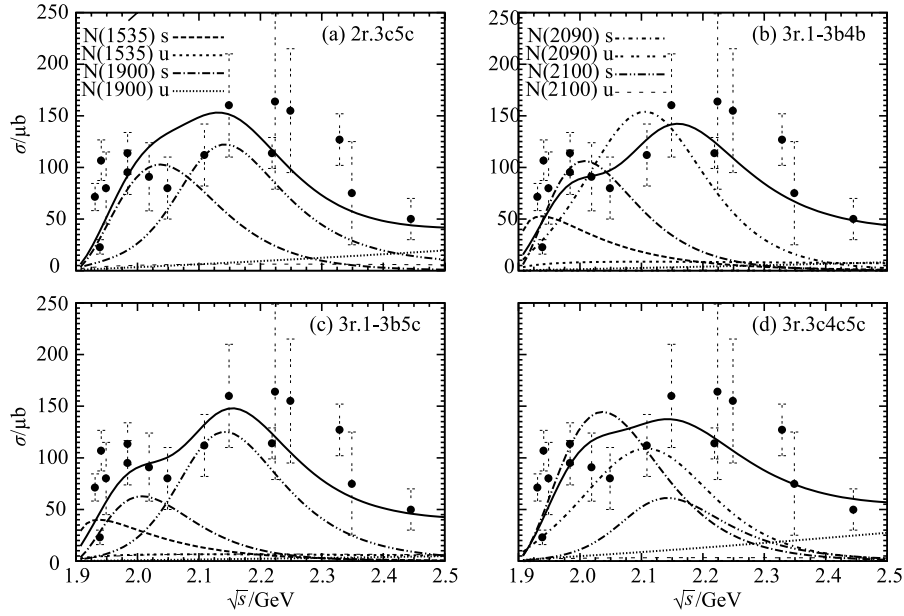


Fig. 4. Selected diagrammatic representation for the fitted results with the combination of two resonances 2r.3c5c and three resonances 3r.1-3b4b, 3r.1-3b5c and 3r.3c4c5c, see Table 3 for the corresponding parameters. The solid lines are the total contributions of all considered diagrams. The explanation of the meaning of other lines in the figures is indicated in (a) and (c). The data are from the compilation [64].

Regarding the four-resonance solutions, besides those mentioned above including the $P_{11}(1710)$ (see Fig. 3(c) for a representative example), the $S_{11}(1535)$, $P_{13}(1900)$, $S_{11}(2090)$ and $P_{11}(2100)$ together could reproduce the data, as listed in Table 4. The χ^2 ranges from 2.1 to 2.5 depending on the different widths of three resonances above threshold and the wider widths seem to be slightly favored, mainly because of the feature of the data mentioned above. The contribution of $S_{11}(1535)$ is prominent in the close-to-threshold region, as can be seen in Fig. 5. The $P_{13}(1900)$ is responsible for the first bump while the $S_{11}(2090)$ and $P_{11}(2100)$ together produce the second one. This also happens in many other solutions when they are included.

It can be seen the situation is much more complicated than that in the $\pi^- p \rightarrow \phi n$ channel, where the $S_{11}(1535)$ resonance is dominant in a wide energy range [60]. But we can still find some common features in all the solutions besides those mentioned above. The contribution of the u-channel $S_{11}(1535)$ and $P_{11}(2100)$ is moderate at all energies and the u-channel $P_{11}(1900)$ is important at high energies. The u-channel $S_{11}(2090)$ term is very small and tends to be negligible. The interference effect can be seen, especially at threshold range, but it is not so important. This is understandable because we only fit the total cross section but the interference effect is more obvious in the differential cross sections and polarization observables. Moreover, it should be pointed out that the large errors of the relative phase ϕ_u , most of which are compatible with zero, reflect the smallness of the corre-

sponding u-channel contribution, but not only because of the limited data base.

Based on the above analysis, we can conclude that at least one of the resonances among the $S_{11}(1535)$, $P_{11}(1710)$ and $P_{11}(1900)$ is required by the close-to-threshold data. We can also safely draw the conclusion that at least one relatively broad resonance above $\eta'N$ threshold is preferred. The data of total cross sections alone are obviously not sufficient to reliably extract the information of the resonances and model parameters, so the above demonstrated solutions are just several possibilities for description of the present data. It is possible to further pin down the model parameters by more accurate data, e.g. differential cross sections, which are however not at hand. It seems that the data of η' photoproduction would give more constraints for the model parameters, especially the masses and widths of the contributed resonances, as done by Huang et al. [55]. Anyway, the central values of extracted coupling constants are quite stable within the given uncertainties among these solutions, as shown in the tables. Especially, our present $g_{\eta'NN^*(1535)}$ is consistent with the values in Ref. [30], and gives further support to the idea that the wave function of $N^*(1535)$ resonance has a large $s\bar{s}$ component [61, 62]. These reasons give us the confidence to use the extracted information from the $\pi N \rightarrow \eta'N$ reaction to study the $J/\psi \rightarrow p\bar{p}\eta'$ decay.

The BES Collaboration has accurately measured $BR(J/\psi \rightarrow p\bar{p}\eta')$ to be $(2.00 \pm 0.23 \pm 0.28) \times 10^{-4}$ [43], about one order of magnitude smaller than that

of the $J/\psi \rightarrow p\bar{p}\eta$ channel. With the total width $\Gamma_{J/\psi} = 92.9 \pm 2.8$ keV [1], we know the corresponding $\Gamma_{J/\psi \rightarrow p\bar{p}\eta'} = (1.86 \pm 0.27 \pm 0.32) \times 10^{-2}$ keV. The calculated $\Gamma_{J/\psi \rightarrow p\bar{p}\eta'}$ using the above parameters is in the range of

$(0.9 - 8.2) \times 10^{-2}$ keV, roughly compatible with the experiment within errors. These results confirm the reliability of our choice of the cut-off values in the form factors and the extracted coupling constants.

Table 4. The coupling constants of nucleon resonances to $\eta'N$ and relative phases extracted in the fit with the combination of four resonances, see the text for details. *: The values are set to be zero in the fit.

label/ χ^2	N*	width	$g_{\eta'NR}$	$\phi_s/(\circ)$	$\phi_u/(\circ)$
4r.1-3a4b5b	1535	—	5.54 ± 2.88	0.0*	0.0 ± 71.8
	1900	(a)	14.88 ± 1.67	0.0 ± 36.1	182.8 ± 47.7
	2090	(b)	1.11 ± 0.49	251.2 ± 46.7	0.0 ± 349.1
	2.50	2100	4.21 ± 2.34	78.5 ± 50.6	0.0 ± 36.2
4r.1-3a4b5c	1535	—	2.63 ± 1.09	0.0*	160.5 ± 63.2
	1900	(a)	15.17 ± 2.45	8.0 ± 29.4	333.3 ± 76.5
	2090	(b)	1.28 ± 0.42	292.6 ± 23.7	147.5 ± 114.2
	2.46	2100	3.66 ± 2.01	325.1 ± 33.7	157.0 ± 46.0
4r.1-3a4c5c	1535	—	3.36 ± 1.48	0.0*	163.2 ± 76.1
	1900	(a)	14.39 ± 2.60	323.3 ± 59.6	0.0 ± 50.2
	2090	(c)	1.90 ± 0.74	283.3 ± 35.8	158.1 ± 121.0
	2.38	2100	3.09 ± 2.85	357.8 ± 358.5	134.8 ± 85.7
4r.1-3b4b5b	1535	—	3.78 ± 2.58	0.0*	52.5 ± 92.1
	1900	(b)	13.17 ± 1.13	0.0 ± 240.6	239.4 ± 98.3
	2090	(b)	1.29 ± 0.58	252.9 ± 30.0	54.8 ± 281.3
	2.23	2100	2.42 ± 2.81	188.3 ± 258.0	65.2 ± 101.9
4r.1-3b4b5c	1535	—	5.55 ± 4.67	0.0*	347.7 ± 53.2
	1900	(b)	12.0 ± 1.14	286.6 ± 65.3	194.9 ± 61.5
	2090	(b)	1.05 ± 0.51	210.7 ± 73.1	346.5 ± 61.9
	2.39	2100	3.19 ± 3.29	9.2 ± 20.2	348.3 ± 5.5
4r.1-3b4c5b	1535	—	5.62 ± 3.16	0.0*	0.0 ± 47.4
	1900	(b)	12.50 ± 1.34	0.0 ± 61.4	196.2 ± 63.1
	2090	(c)	1.68 ± 0.66	251.7 ± 37.5	19.7 ± 226.7
	2.19	2100	3.34 ± 2.81	91.8 ± 77.4	36.2 ± 70.0
4r.1-3b4c5c	1535	—	4.50 ± 3.75	0.0*	0.0 ± 38.7
	1900	(b)	12.51 ± 1.55	0.0 ± 70.3	189.4 ± 73.9
	2090	(c)	1.43 ± 0.96	240.5 ± 62.4	13.6 ± 281.4
	2.17	2100	4.01 ± 3.17	92.4 ± 86.1	31.3 ± 65.9
4r.1-3c4c5c	1535	—	3.62 ± 2.78	0.0*	0.0 ± 271.5
	1900	(c)	9.76 ± 1.59	0.0 ± 305.4	196.9 ± 133.8
	2090	(c)	1.44 ± 1.33	226.6 ± 50.4	88.7 ± 214.3
	2.12	2100	3.88 ± 2.77	123.1 ± 94.3	99.3 ± 97.5

What we are more interested in is the invariant mass spectra and Dalitz plots, which may give us insight into the information of nucleon resonances. In Fig. 6 we show the invariant mass spectra of the solutions 3r.2-3b4c, 3r.3c4c5c, 4r.1-3b4c5c and 5r.1-2-3c4c5c as representative examples. It can be seen in Fig. 6(a) that the calculated spectra do not have significant differences between solutions 3r.2-3b4c and 3r.3c4c5c, and this is also true for solutions 4r.1-3b4c5c and 5r.1-2-3c4c5c in Fig. 6(c)(d). In the $\eta'p$ spectra, the enhancement is usually located above 2.0 GeV and the resonances below threshold move it a little closer to 2.0 GeV, as shown in Fig. 6(a). The more obvious effect of the resonances below threshold appears in the $p\bar{p}$ spectra in Fig. 6(b). So in this situation it is probable to disentangle the two $\eta'N$ production mechanisms mentioned in the Introduction:

the above or below threshold resonant contribution. Figure 7 depicts the Dalitz plots of the solutions 3r.3c4c5c and 5r.1-2-3c4c5c, which agrees with the conclusions in the invariant mass spectra. As can be seen, the $p\bar{p}\eta'p$ plots show more difference between the various solutions so they are more suitable to study the $\eta'N$ production. Unfortunately, some of the invariant mass spectra and Dalitz plots, e.g. solutions 2r.3a5c and 4r.1-3a4b5b, are very close to those of pure phase space, so they are unlikely to be distinguished from the totally non-resonant $\eta'N$ production mechanism. However, we could still expect that these two mechanisms would be recognized in the $\pi N \rightarrow \eta'N$ or $\gamma N \rightarrow \eta'N$ reaction. At present, the data of the $NN \rightarrow NN\eta'$ reaction are mainly in the close-to-threshold range [66, 67] so they should be helpful for fixing the parameters of near-threshold resonances. Our

previous study has found that a S_{11} state, namely the $N^*(1535)$ resonance, could explain both cross sections and invariant spectrum of this channel [30]. As a result, it is interesting to give a combined analysis of the data of various $\eta'N$ production channels in order to pin down the $\eta'N$ production mechanism.

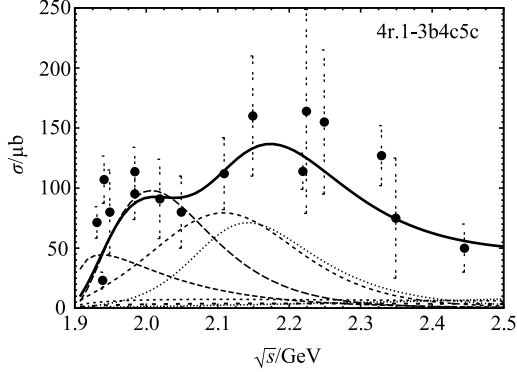


Fig. 5. Representative diagram for the fitted results with the combination of four resonances, e.g. 4r.1-3b4c5c, see Table 4 for the corresponding parameters. The meaning of the lines is the same as those in Fig. 4. The data are from the compilation [64].

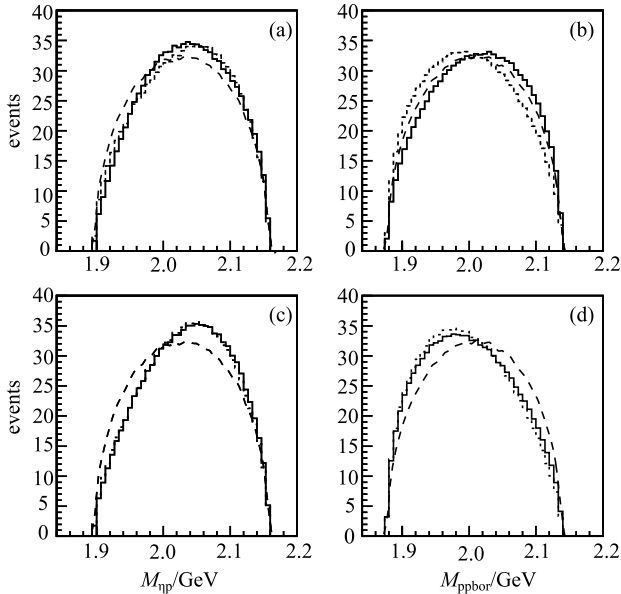


Fig. 6. The invariant mass spectra for the $J/\psi \rightarrow p\bar{p}\eta'$ decay in the isobar model. The dashed curves are the pure phase space distributions. The solid and dashed histograms are for 3r.2-3b4c and 3r.3c4c5c respectively in (a) and (b), while for 4r.1-3b4c5c and 5r.1-2-3c4c5c in (c) and (d).

An updated analysis of the available data of the $\pi N \rightarrow \eta'N$, $\gamma N \rightarrow \eta'N$ and $NN \rightarrow NN\eta'$ reactions has been

done in Ref. [55], which uses the same type of Lagrangians as ours. They include a four-star $P_{13}(1720)$ state, a one-star $P_{11}(2130)$ state, and two other states $S_{11}(1925)$ and $P_{13}(2050)$ which are not listed in the PDG compilation [1]. The total Breit-Wigner widths of these states are all narrower than 210 MeV and their branching ratios of the $\eta'N$ channel are only several percent. It should be noted that their description of the high energy data of the $\pi N \rightarrow \eta'N$ is not so good as our results. If we assume that the coupling of all these states in Ref. [55] to the J/ψ are at the same level, e.g. $g_{\psi NR}^2 = 1.0 \times 10^{-5}$ as indicated in Table 1, then the invariant mass spectra and Dalitz plots could be calculated in Fig. 8 with the extracted parameters from the Table 3 in Ref. [55]. The bumps at the location of $S_{11}(1925)$ and $P_{13}(2050)$ can be clearly seen. The sub-threshold $P_{13}(1720)$ state serves as a smooth background, similar to the role of $P_{11}(1710)$ in our own solutions. The $P_{11}(2130)$ is located at the upper bound of the phase space so its effect is not significant. These distributions are obviously distinguishable from our results so they would be hopefully tested by the future $J/\psi \rightarrow p\bar{p}\eta'$ data.

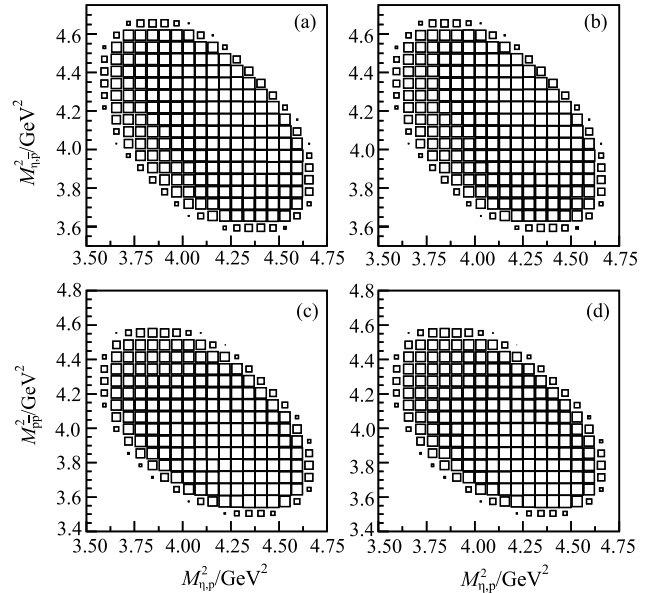


Fig. 7. The Dalitz plots for the $J/\psi \rightarrow p\bar{p}\eta'$ decay in the isobar model. (a) and (b) are for 3r.3c4c5c, while (c) and (d) are for 5r.1-2-3c4c5c.

It seems that it is more difficult to study the resonances in the $J/\psi \rightarrow p\bar{p}\eta'$ channel than in other decay channels, because all the above solutions do not show extraordinary resonance structures in their invariant mass spectra and their deviation from phase space is not very significant. This is contrary to the case in the $J/\psi \rightarrow p\bar{p}\phi$ [60], the $J/\psi \rightarrow p\bar{p}\pi^0$ [36] and the $\psi(3686) \rightarrow p\bar{p}\pi^0$ decays [38], where the resonance peaks appear clearly in the invariant mass spectra and are also

directly reflected in the Dalitz plots. Fortunately, the BESIII group is planning to collect around ten billion J/ψ events in the near future, which is estimated to contain about two million of $J/\psi \rightarrow p\bar{p}\eta'$ decay events. Owing to such a large data sample, it should be possible to study the nucleon resonances in the $J/\psi \rightarrow p\bar{p}\eta'$ decay.

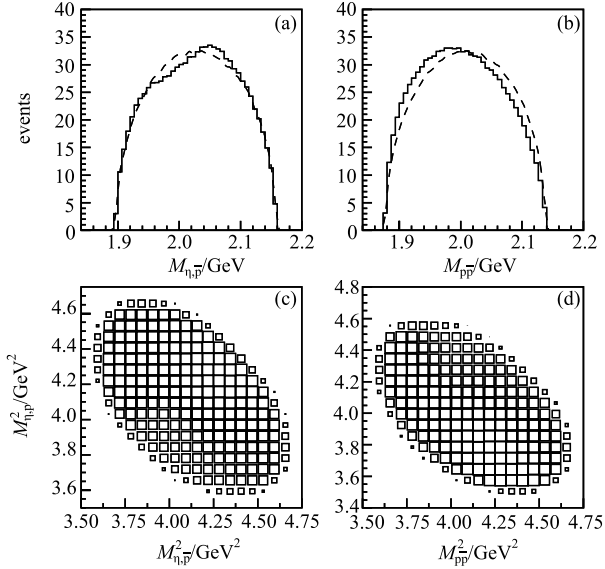


Fig. 8. The invariant mass spectra (a) and (b) and Dalitz plots (c) and (d) for the $J/\psi \rightarrow p\bar{p}\eta'$ decay in the isobar model with the parameters from the Table 3 in Ref. [55].

4 Summary

To summarize, we performed a full analysis in the effective Lagrangian approach to extract the information from the data of $\pi N \rightarrow \eta' N$ reactions. Though the present data do not restrict the production mechanism enough, we find that either a subthreshold resonance or a broad P-wave state at near threshold seems to be required and at least one broad resonance above $\eta' N$ threshold is preferred by the data. This is useful for

our understanding of the nucleon resonances coupling strongly to the $\eta' N$ channel. From the present analysis of the data, we can calculate the $J/\psi \rightarrow p\bar{p}\eta'$ decay and find that there are no such distinct resonance structures in the invariant mass spectra as in other decay channels. However, the $J/\psi \rightarrow p\bar{p}\eta'$ decay may still be useful for discriminating the below- or above-resonance contribution in $\eta' N$ production. The BESIII group are encouraged to do the PWA on the basis of the future large data sample. The data of $\pi N \rightarrow \eta' N$ and $\gamma N \rightarrow \eta' N$ reactions are also suggested to be included to give a combined analysis in order to finally determine the $\eta' N$ production mechanism and resonance contributions, though the photoproduction reactions are complicated by large contributions of the t -channel and contact terms. The new photoproduction data are expected to come soon from the CLAS and CBELSA collaborations, and the updated combined analysis as done in Ref. [55] by inclusion of these new data is encouraged. These would be helpful to reduce the ambiguity in extracting the resonance contents and parameters and so reinforce our understanding of the η' -meson production mechanism.

Our results are enlightening for the $\eta' N$ production mechanism and the properties of the nucleon resonances with mass around 2.0 GeV. It is worth pointing out that our results are also meaningful for the study of the $p\bar{p} \rightarrow J/\psi \eta'$ at PANDA@FAIR [65]. We can speculate that the contribution of the t -channel nucleon resonances should be much more important than that of the t -channel nucleon pole in this reaction. A similar conclusion should be also applied to the associate production of charmonium states and other non-strange mesons (except for the π -meson) in $p\bar{p}$ annihilation, namely $p\bar{p} \rightarrow J/\psi \eta$, $p\bar{p} \rightarrow J/\psi \omega$ and $p\bar{p} \rightarrow J/\psi \phi$. As a result, the total cross section of these reactions are expected to be enhanced so they could be more easily measured at PANDA.

We would like to thank Dr. J. P. Dai and Prof. B. S. Zou for useful discussions.

References

- 1 J. Beringer et al (Particle Data Group), Phys. Rev. D, **86**: 010001 (2012); K. A. Olive et al (Particle Data Group), Chin. Phys. C, **38** (9): 090001 (2014)
- 2 A. V. Anisovich, E. Klempt, V. A. Nikonov et al, Eur. Phys. J. A, **47**: 27 (2011)
- 3 A. V. Anisovich, R. Beck, E. Klempt et al., Eur. Phys. J. A, **48**: 15 (2012)
- 4 V. A. Nikonov, A. V. Anisovich, E. Klempt et al., Phys. Lett. B, **662**: 245–251 (2008)
- 5 A. V. Anisovich, E. Klempt, V. A. Nikonov et al., Phys. Lett. B, **711**: 167–172 (2012)
- 6 T. Feuster and U. Mosel, Phys. Rev. C, **58**: 457–488 (1998); **59**: 460–491 (1999)
- 7 G. Penner and U. Mosel, Phys. Rev. C, **66**: 055211 (2002); **66**: 055212 (2002)
- 8 V. Shklyar, G. Penner, and U. Mosel, Eur. Phys. J. A, **21**: 445–454 (2004)
- 9 V. Shklyar, H. Lenske, U. Mosel, and G. Penner, Phys. Rev. C, **71**: 055206 (2005)
- 10 V. Shklyar, H. Lenske, and U. Mosel, Phys. Rev. C, **72**: 015210 (2005)
- 11 V. Shklyar, H. Lenske, and U. Mosel, Phys. Lett. B, **650**: 172–178 (2007)
- 12 V. Shklyar, H. Lenske, and U. Mosel, Phys. Rev. C, **87**: 015201 (2013)
- 13 X. Cao, V. Shklyar, and H. Lenske, Phys. Rev. C, **88**: 055204 (2013)
- 14 D. M. Manley and E. M. Saleski, Phys. Rev. D, **45**: 4002–4033

- (1992)
- 15 M. Shrestha and D. M. Manley, *Phys. Rev. C*, **86**: 055203 (2012)
 - 16 R. L. Workman, W. J. Briscoe, and M. W. Paris et al, *Phys. Rev. C*, **85**: 025201 (2012)
 - 17 M. Döring, C. Hanhart, and F. Huang et al, *Nucl. Phys. A*, **851**: 58–98 (2011)
 - 18 F. Huang, M. Döring, and H. Haberzettl et al, *Phys. Rev. C*, **85**: 054003 (2012)
 - 19 D. Rönchen, M. Döring, and F. Huang et al, *Eur. Phys. J. A*, **49**: 44 (2013)
 - 20 A. Matsuyama, T. Sato, and T.-S. H. Lee, *Phys. Rep.*, **439**: 193–253 (2007)
 - 21 H. Kamano, S. X. Nakamura, T.-S. H. Lee, and T. Sato, *Phys. Rev. C*, **88**: 035209 (2013)
 - 22 H. Kamano, *Phys. Rev. C*, **88**: 045203 (2013)
 - 23 B. C. Liu and B. S. Zou, *Phys. Rev. Lett.*, **96**: 042002 (2006)
 - 24 J. J. Xie and B. S. Zou, *Phys. Lett. B*, **649**: 405–412 (2007)
 - 25 J. J. Xie, B. S. Zou, and H. C. Chiang, *Phys. Rev. C*, **77**: 015206 (2008)
 - 26 J. J. Xie and C. Wilkin, *Phys. Rev. C*, **82**: 025210 (2010)
 - 27 J. J. Xie, H. X. Chen, and E. Oset, *Phys. Rev. C*, **84**: 034004 (2011)
 - 28 J. J. Xie and B. C. Liu, *Phys. Rev. C*, **87**: 045210 (2013)
 - 29 X. Cao, X. G. Lee, and Q. W. Wang, *Chin. Phys. Lett.*, **25**: 888 (2008)
 - 30 X. Cao and X. G. Lee, *Phys. Rev. C*, **78**: 035207 (2008)
 - 31 X. Cao, J. J. Xie, B. S. Zou, and H. S. Xu, *Phys. Rev. C*, **80**: 025203 (2009)
 - 32 X. Cao, *Chin. Phys. C*, **33**: 1381–1384 (2009)
 - 33 X. Cao, B. S. Zou, and H. S. Xu, *Phys. Rev. C*, **81**: 065201 (2010)
 - 34 X. Cao, B. S. Zou, and H. S. Xu, *Nucl. Phys. A*, **861**: 23–36 (2011)
 - 35 X. Cao, B. S. Zou, and H. S. Xu, *Int. J. Mod. Phys. A*, **26**: 505–510 (2011)
 - 36 M. Ablikim et al (BES Collaboration), *Phys. Rev. D*, **80**: 052004 (2009)
 - 37 M. Ablikim et al (BES Collaboration), *Phys. Rev. Lett.*, **97**: 062001 (2006)
 - 38 M. Ablikim et al (BES Collaboration), *Phys. Rev. Lett.*, **110**: 022001 (2013)
 - 39 M. Ablikim et al (BES Collaboration), *Phys. Rev. D*, **74**: 012004 (2006)
 - 40 J. Z. Bai et al (BES Collaboration), *Phys. Lett. B*, **510**: 75–82 (2001)
 - 41 H. X. Yang et al (BES Collaboration), *Int. J. Mod. Phys. A*, **20**: 1985–1989 (2005)
 - 42 M. Ablikim et al (BES Collaboration), *Phys. Lett. B*, **659**: 789–795 (2008)
 - 43 M. Ablikim et al (BES Collaboration), *Phys. Lett. B*, **676**: 25–30 (2009)
 - 44 M. Ablikim et al (BES Collaboration), *Phys. Rev. D*, **87**: 112004 (2013)
 - 45 R. A. Briere et al (CLEO Collaboration), *Phys. Rev. Lett.*, **95**: 062001 (2005)
 - 46 S. B. Athar et al (CLEO Collaboration), *Phys. Rev. D*, **75**: 032002 (2007)
 - 47 B. S. Zou and D. V. Bugg, *Eur. Phys. J. A*, **16**: 537–547 (2003)
 - 48 B. S. Zou and F. Hussain, *Phys. Rev. C*, **67**: 015204 (2003)
 - 49 S. Dulat and B. S. Zou, *Eur. Phys. J. A*, **26**: 125–134 (2005)
 - 50 K. P. Khemchandani, A. Martínez Torres, H. Nagahiro, and A. Hosaka, *Phys. Rev. D*, **88**: 114016 (2013)
 - 51 E. Oset and A. Ramos, *Phys. Lett. B*, **704**: 334–342 (2011)
 - 52 K. Nakayama, H. F. Arellano, J. W. Durso, and J. Speth, *Phys. Rev. C*, **61**: 024001 (1999)
 - 53 K. Nakayama and H. Haberzettl, *Phys. Rev. C*, **69**: 065212 (2004)
 - 54 K. Nakayama and H. Haberzettl, *Phys. Rev. C*, **73**: 045211 (2006)
 - 55 F. Huang, H. Haberzettl, and K. Nakayama, *Phys. Rev. C*, **87**: 054004 (2013)
 - 56 W. H. Liang, P. N. Shen, J. X. Wang, and B. S. Zou, *J. Phys. G*, **28**: 333–343 (2002)
 - 57 W. H. Liang, P.-N. Shen, B.-S. Zou, and A. Faessler, *Eur. Phys. J. A*, **21**: 487–500 (2004)
 - 58 T. Barnes, X. Li, and W. Roberts, *Phys. Rev. D*, **81**: 034025 (2010)
 - 59 R. Sinha and S. Okubo, *Phys. Rev. D*, **30**: 2333 (1984)
 - 60 J. P. Dai, P. N. Shen, J. J. Xie, and B. S. Zou, *Phys. Rev. D*, **85**: 014011 (2012)
 - 61 C. S. An and B. S. Zou, *Sci. Sin. G*, **52**: 1452–1457 (2009)
 - 62 C. S. An and B. Saghai, *Phys. Rev. C*, **84**: 045204 (2011)
 - 63 J. Shi, J. P. Dai, and B. S. Zou, *Phys. Rev. D*, **84**: 017502 (2011)
 - 64 A. Baldini, V. Flamino, W. G. Moorhead, and D. R. O. Morrison, *Total Cross Sections of High Energy Particles* (Landolt-Bornstein: Numerical Data and Functional Relationships in Science and Technology, vol. 12, edited by H. Schopper: Springer-Verlag, Berlin, 1988)
 - 65 Q. Y. Lin, H. S. Xu, and X. Liu, *Phys. Rev. D*, **86**: 034007 (2012)
 - 66 E. Czerwiński et al, *Phys. Rev. Lett.*, **113**: 062004 (2014)
 - 67 P. Klaja et al, *Phys. Lett. B*, **684**: 11–16 (2010)